

L. Kalmár, Ph.D., University of Miskolc, Hungary,  
 G. Janiga, Ph.D. Dr. habil, Otto -von Guericke University of Magdeburg, Germany  
 L. Soltész, MSc, Electrolux Lehel Ltd., Small Appliance Factory, Hungary

## CHARACTERISATION OF DIFFERENT ONE-STAGE BLOWER CONFIGURATIONS USING 3D UNSTEADY NUMERICAL FLOW SIMULATIONS

*This paper deals with the CFD investigation of the flow in a one-stage radial flow blower-aggregate. The main aim of this numerical study is to compute the relevant operating characteristics of the blower-aggregate and to determine detailed information about the flow characteristics inside it. The distributions of these flow characteristics in the blower determined by the commercial code ANSYS-FLUENT [1] are available to judge whether the elements of the blower are working properly, or not. The calculated characteristics of operating parameters are compared in this paper with measured data given by experimental tests of the blower-aggregate for their validation [2]. The blower-aggregates investigated numerically are noted by  $BA_1$ ,  $BA_2$  and  $BA_3$  in this paper.*

### 1. INTRODUCTION

The investigated blower aggregate can be seen in Figure 1 and the same aggregate is shown in Figure 2 in a disassembled state to introduce the main parts of the blower. The first step of our numerical investigation was to create the complete computational domain of the blower-aggregate. It has been produced in the commercial pre-processing tool ANSYS-GAMBIT. The entire three-dimensional computational domain of the blower aggregate is illustrated in Figure 3 in two different views. By comparing the photos of the blower (see Figures 1 and 2) and the 3D drawing of the aggregate model (see Figure 3) it is easy to realise that the inlet and outlet parts of the model are slightly modified.

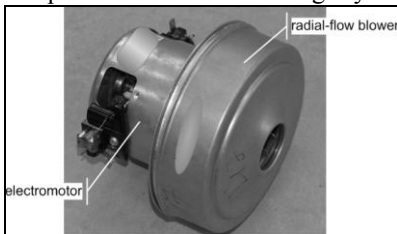


Figure 1 – Photo of the investigated blower aggregate  $BA_1$

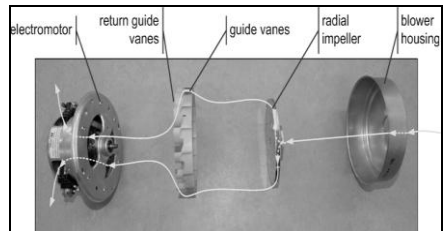


Figure 2 – Main components of the blower aggregate  $BA_1$

At the inlet cross section of the blower – to produce relatively homogenous velocity distribution along the inlet cross section during the numerical simulation – a cylindrical short pipe section with circular cross section was connected. At the outlet section of the blower two short cylindrical pipe sections were connected with the similar shape of the cross section which can be seen in the wall between the blower and electromotor (see Figure 2).

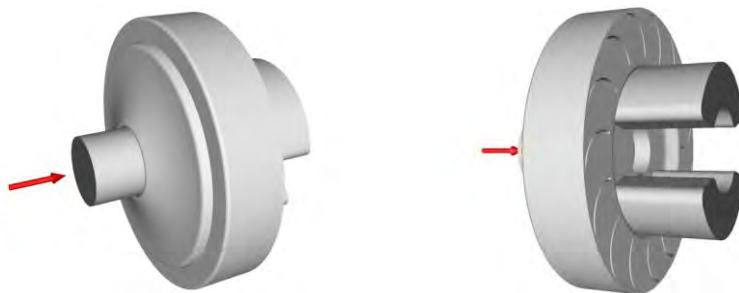


Figure 3 – The three-dimensional computational domain of the blower aggregate  $BA_1$

In Figure 3 the inlet-, outlet sections and the house of the blower can be seen. During the numerical simulation the total 3D computational domain (see Figure 3) also contains the rotating impeller (see Figure 4) and the stationary guide vanes and the stationary return guide vanes (see Figure 5) of the blower, which can be found inside the blower house.



Figure 4 – The three-dimensional computational domain of the impeller of the blower aggregate  $BA_1$

The air flows into the blower throughout the inlet section and arrives to the impeller, then flows across it which increases the total energy of the air. After first the air flows in the guide vanes at impeller side then flows in the guide vanes on the back side. Finally the air flows through the pressured side of the blower and leaves the blower throughout the outlet sections. The main aim of this numerical investigation is to determine the relevant operating characteristics of the blower by CFD numerical methods.

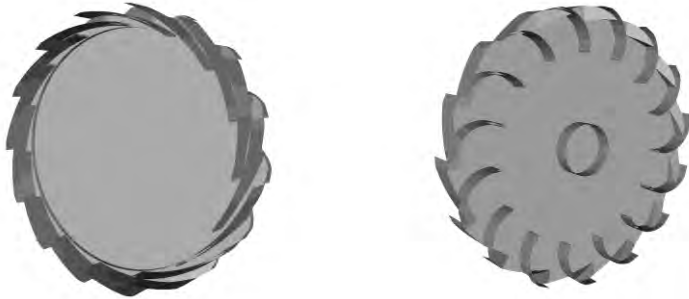


Figure 5 – The three-dimensional computational domain of the guide vanes of the blower aggregate *BAI*

## 2. COMPUTATIONAL CONFIGURATION

To carry out the numerical simulation of flow in blower, the total computational domain has to be divided into sub domains, as shown in Figure 6. Two types of important sub-domains have to be detached because of their operations: the rotational sub-domain (named **ROTOR**) is the sub-domain of the blower impeller and the stationary sub-domains (named **STATOR**) which are bounded by the walls of the blower, the guide vanes and return guide vanes.

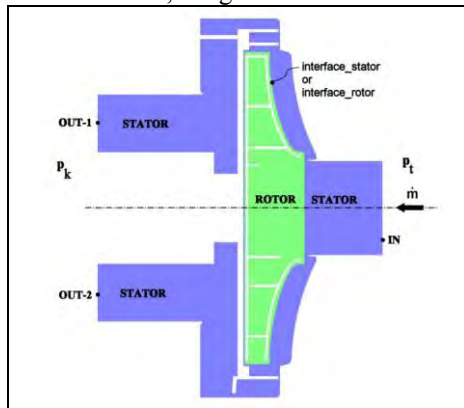


Figure 6 – Partitioning of the computational domain

## 3. COMPUTATIONAL METHODS

The finite volume method is applied to determine the solution of the flow problems by FLUENT. That is why before starting to run the code all the sub-domains have to be divided into finite volumes. In other words, we have to mesh the total computational domain. When carrying out this procedure we have to pay extra attention to the geometrical characteristics of each finite element. The mesh generation was carried out with the commercial code ANSYS-GAMBIT. To get information about the quality of mesh elements it is the most convenient way to

display the actual values of the cells skewness. In our case 5.03 million cells were developed and the measured maximum value was equal to 0.8082, which means that the quality of the meshing is acceptable to perform the CFD computation of the flow in blower aggregate  $BA_I$ . Some details of the computational mesh of the impeller are illustrated in Figure 7.

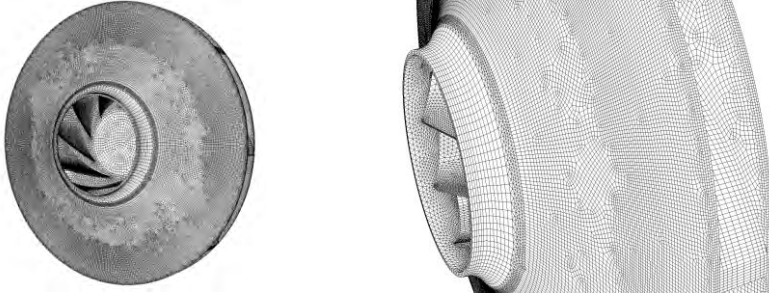


Figure 7 – The computational mesh of the impeller surface of the blower aggregate  $BA_I$

#### 4. COMPUTATIONAL RESULTS

For all the cells of the total computational domain the “density based implicit Gauss-Seidel” numerical solver was used during the numerical solution process assuming unsteady flow. Because during the operations of blower relatively high velocities and pressures increase take place, it was also supposed that the fluid was compressible and viscous. In this way the standard  $k-\omega$  SST turbulent models and perfect-gas law were applied in our simulations. The computational results obtained by Fluent are illustrated next. Figures 9 and 10 show the local distributions of the velocity and absolute or dynamic pressure fields, while all the diagrams give information about the variations of average absolute or dynamic pressure, density and the mass-flow (concerning to the denoted 16 different sections of the flow in Figure 8) in direction of the main flow inside the aggregate.

Figures 9-12 give insight into the local structures of the flow using streamlines along the two planes denoted by A and B. By using our developed numerical model three different planes operating points of the blower aggregate  $BA_I$  were numerically investigated by Fluent. One of the initial parameters of our calculation was the mass-flow rate at inlet, and the actual pressure difference between the outlet and inlet sections of the blower was calculated in this way. For validation of our calculation we compared the characteristics of three calculated working points determined separately by actual values of the mass flow rates  $\dot{m}_I=0.046$  kg/s,  $\dot{m}_{II}=0.033$  kg/s and  $\dot{m}_{III}=0.022$  kg/s with the measured characteristic curve of the blower aggregate  $BA_I$  given by laboratory tests [2], which are shown in Figure 13. A very good agreement can be observed in this figure.

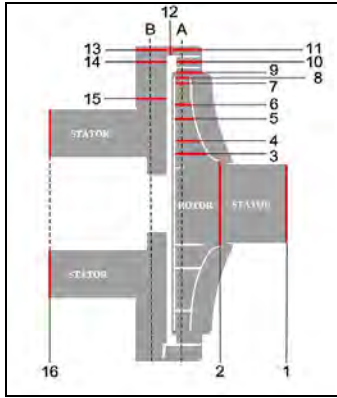


Figure 8 – Positions of sections 1-16 of the flow and two planes of **A** and **B**

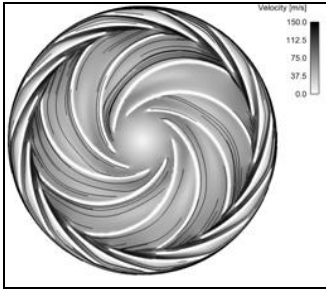


Figure 9 – Velocity field along plane **A** of the blower aggregate **BA<sub>1</sub>**

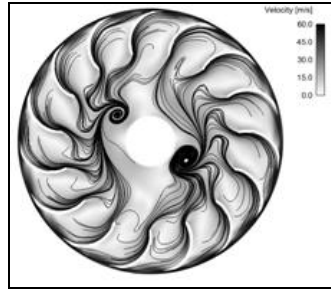


Figure 10 – Velocity field along plane **B** of the blower aggregate **BA<sub>1</sub>**

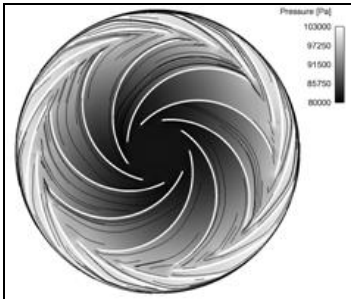


Figure 11 – Absolute pressure field along plane **A** of the blower aggregate **BA<sub>1</sub>**

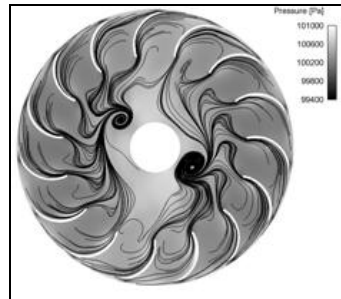


Figure 12 – Absolute pressure field along plane **B** of the blower aggregate **BA<sub>1</sub>**

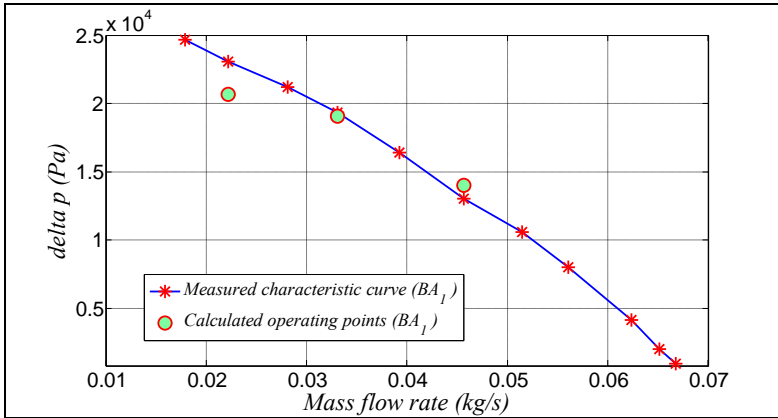


Figure 13 – Calculated working points and measured characteristic curve of the blower aggregate **BA<sub>1</sub>**

The CFD investigations introduced above are also carried out for additional two different blower aggregates noted by **BA<sub>2</sub>** and **BA<sub>3</sub>**. The blower aggregates **BA<sub>2</sub>** and **BA<sub>3</sub>** are very similar to blower aggregate **BA<sub>1</sub>**, except the following differences:

- the blower aggregate **BA<sub>2</sub>** has newly designed stationary guide vanes and the stationary return guide vanes with new geometries,
- the blower aggregate **BA<sub>3</sub>** has newly designed radial flow impeller, redesigned stationary guide vanes and the stationary return guide vanes with new geometries.

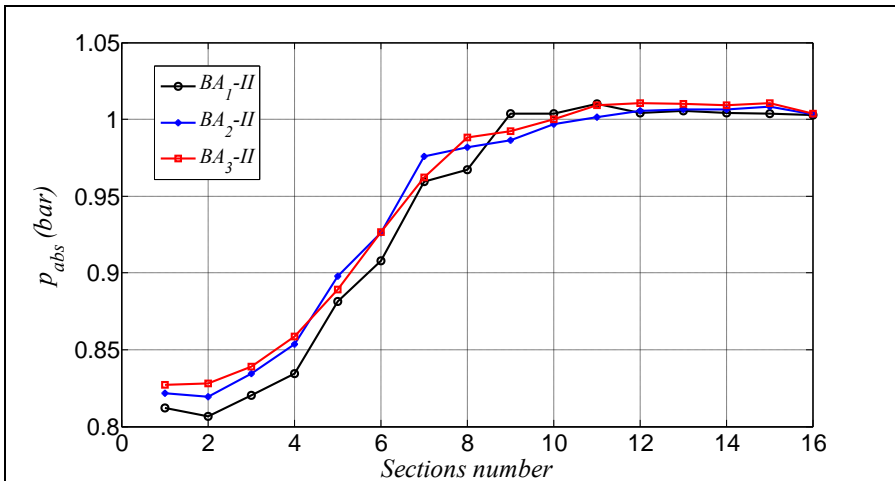


Figure 14 – Variation of absolute pressure

Figures 14-17 show the variations of averaged flow parameters which are determined by surface integration of physical fields concerning the blower aggregates  $BA_1$ ,  $BA_2$  and  $BA_3$ . All of them are determined for operation state at mass flow rate  $\dot{m}_{II}=0.033$  kg/s for all of the blower aggregates.

Knowing the variations of these averaged parameters is very important, if we want to get useful information about the operational characteristics of the blower. The sixteen different cross-sections can be seen (see Figure 8). The average values of absolute, dynamic pressures and density were determined by surface integration for the denoted 16 sections and the variations of these flow characteristics are shown in Figures 14, 15 and 16. The values of mass flow rate concerning these cross sections are also calculated and shown in Figure 17.

In this way in Figures 14 and 15 between sections 2 and 8 (inside the impeller) the variations of absolute and dynamic pressure show the energy increase through the impeller. Between sections 8 and 10 the increase in cross sectional area causes a sudden drop in the dynamic pressure and a small increase in the absolute pressure. In Figure 17 between sections 2 and 8 the relatively large increase caused by leakage.

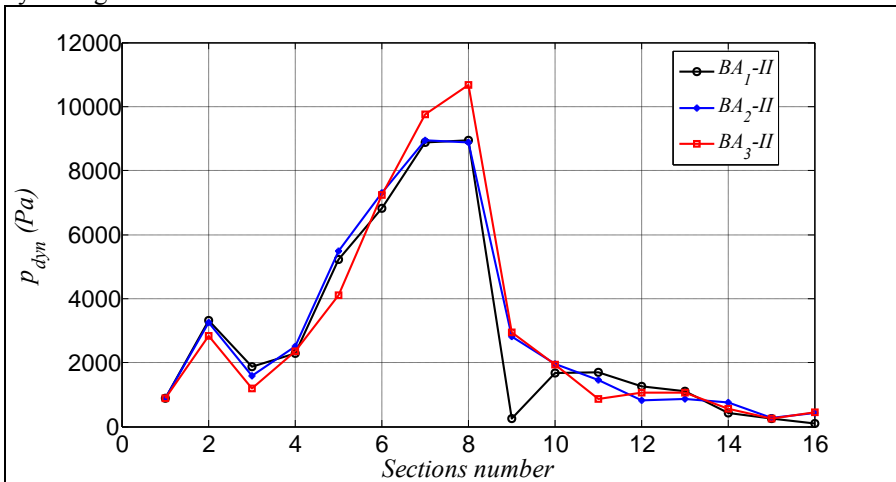


Figure 15 – Variation of dynamic pressure

## SUMMARY

This study has demonstrated that numerical flow simulations are able to provide detailed information about the local flow structures supporting the design process. These structures are introduced, e.g., in Fig. 9 illustrating the stagnation surfaces or in Fig. 12 showing the vertical structures in return guide vanes. All these effects diminish the efficiency of the machine; therefore, they should be eliminated as possible.

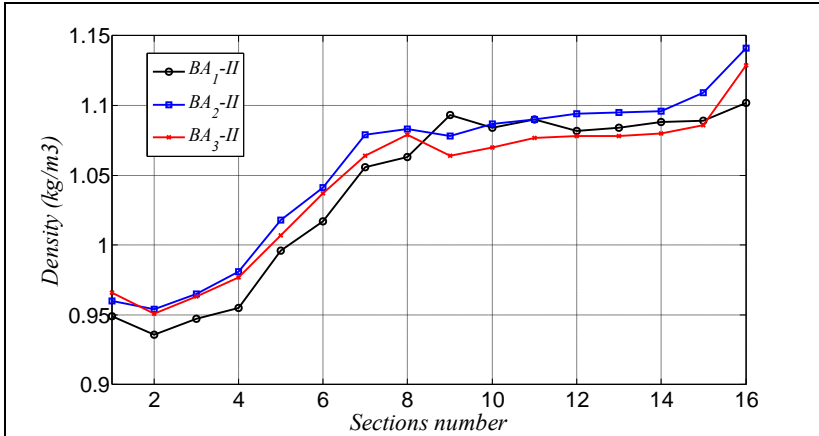


Figure 16 – Variation of air density

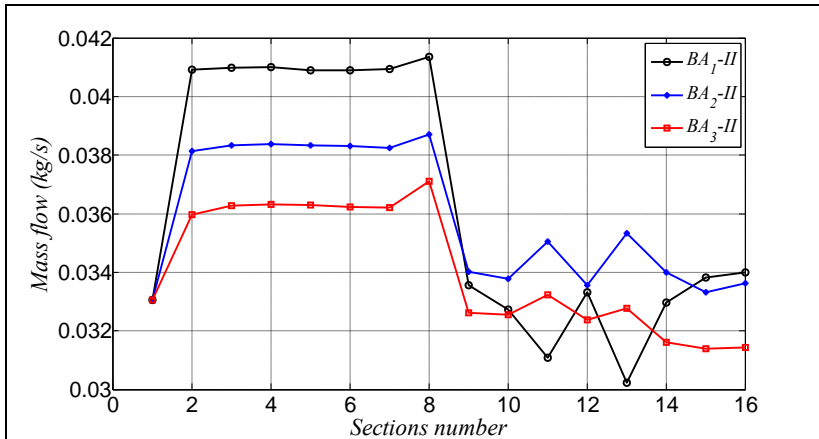


Figure 17 – Variation of mass flow rate

#### ACKNOWLEDGEMENT

The work was carried out as part of the TÁMOP-4.2.1.B-10/2/KONV-2010-0001 project in the framework of the New Hungarian Development Plan. The realization of this project is supported by the European Union, co-financed by the European Social Fund.

**REFERENCES:** [1] Ansys Inc., *ANSYS FLUENT 12.0 User's Guide*, Canonsburg, PA, USA, 2009; [2] Lakatos, K., Szaszák, N., Mátrai Zs., Soltész, L., Szabó, Sz.: **Experimental Development of Guide Vanes and Return Guide Vanes of a Mini Blower**, *Proc. of MicroCAD International Computer Science Conference, Miskolc*, pp. 65-72, 2011.

Поступила в редколлегию 22.05.2012